Title
Ozone photochemical production in urban Shanghai, China: Analysis based on ground level observations

Journal
Journal of Geophysical Research, 114(D15)

ISSN
0148-0227

Authors
Ran, Liang
Zhao, Chunsheng
Geng, Fuhai
et al.

Publication Date
2009

DOI
10.1029/2008jd010752

Ozone photochemical production in urban Shanghai, China: Analysis based on ground level observations

Liang Ran,[1] Chunsheng Zhao,[1] Fuhai Geng,[2] Xuexi Tie,[3] Xu Tang,[2] Li Peng,[2] Guangqiang Zhou,[2] Qiong Yu,[2] Jianmin Xu,[2] and Alex Guenther[3]

Received 9 July 2008; revised 26 May 2009; accepted 3 June 2009; published 1 August 2009.

[1] Ozone and its precursors were measured from 15 June 2006 to 14 June 2007 at an urban site in Shanghai and used to characterize photochemical oxidant production in this region. During the observation period, ozone displays a seasonal variation with a maximum in spring. Observed nitrogen oxides (NOx) and carbon monoxide (CO) reached a maximum in winter and a minimum in summer. NOx and CO has a similar double-peak diurnal cycle, implying that they are largely of motor vehicle origin. Total nonmethane organic compounds (NMOC) concentrations averaged over the morning, and the 24-hour periods have a large day-to-day variation with no apparent seasonal cycle. Aromatics play a dominant role in contributing to total NMOC reactivity and ozone-forming potential. Anthropogenic NMOC of diverse sources are major components of total NMOC and consist mainly of moderate and low reactivity species. In contrast, relatively low levels of biogenic NMOC concentrations were observed in urban Shanghai. The early morning NMOC/NOx ratios are typically below 8:1 with an average of around 4:1, indicating that the sampling location is situated in a NMOC-limited regime. Model simulations confirm that potential photochemical ozone production in Shanghai is NMOC-sensitive. It is presently difficult to predict the impact of future human activities, such as the increase of automobiles and vegetation-covered landscapes and the reduction of aerosol on ozone pollution in the fast developing megacities of China, and additional studies are needed to better understand the highly nonlinear ozone problem.

Citation: Ran, L., C. Zhao, F. Geng, X. Tie, X. Tang, L. Peng, G. Zhou, Q. Yu, J. Xu, and A. Guenther (2009), Ozone photochemical production in urban Shanghai, China: Analysis based on ground level observations, *J. Geophys. Res.*, *114*, D15301, doi:10.1029/2008JD010752.

1. Introduction

[2] Rapid urbanization and industrialization have led to a substantial degradation of air quality in many regions of China. A severe ozone problem has recently risen to be one of the most important urban air quality issues especially in some megacities. Shanghai is a large city in China with a population over 16 million, more than 2 million automobiles, a large number of tall buildings, and a heavily industrialized area on the edge of the metropolitan area. Shanghai and other megacities will continue to expand in response to ongoing economic growth. Knowledge of the processes controlling ozone production and destruction is therefore crucial for effective ozone control strategies. While concerns regarding ozone pollution have been sufficiently addressed in many other megacities in the world [e.g., *Wakamatsu et al.*, 1999; *Jiang and Fast*, 2004; *Qin et al.*, 2004; *Murphy and Allen*, 2005; *Civeroloa et al.*, 2007; *Stephens et al.*, 2008; *Ying et al.*, 2009], few observations are available for Shanghai [*Zhao et al.*, 2004; *Wang et al.*, 2006; *Geng et al.*, 2006]. Concentrations of ozone and its photochemical precursors have not been systemically measured and their relationships are not well known. In this paper, we explore these important issues using an observational data set that is more comprehensive than what has previously been available for Shanghai and model simulations designed to improve understanding of the atmospheric photochemistry in megacities.

[3] Ambient ozone concentration is nonlinear with respect to many influencing factors such as emission distributions, photochemical processes, transport, deposition and meteorology [*Seinfeld*, 1989; *Committee on Tropospheric Ozone Formation and Measurement*, 1991; *Seinfeld and Pandis*, 1998; *Jenkin and Clemitshaw*, 2000; *Trainer et al.*, 2000; *Hidy*, 2000]. The nonlinearity complicates detailed understanding of the ozone problem and development of effective ozone abatement strategies. This is typically addressed by the examination of ambient observations to determine the relative roles of different ozone precursors [*Russell et al.*, 1995; *Qin et al.*, 2004; *Shiu et al.*, 2007; *Zhang et al.*, 2007], that can subsequently guide regulatory

[1]Department of Atmospheric Science, School of Physics, Peking University, Beijing, China.
[2]Pudong Meteorological Bureau, Shanghai Meteorological Administration, Shanghai, China.
[3]Atmospheric Chemistry Division, National Center for Atmospheric Research, Boulder, Colorado, USA.

0148-0227/09/2008JD010752

efforts [*Seinfeld*, 1989; *Chang and Rudy*, 1990; *Chameides et al.*, 1992; *Trainer et al.*, 2000]. The role of nitrogen oxides (NOx) and nonmethane organic compounds (NMOCs) as the major ozone precursors in urban areas has been known since the Los Angeles smog studies led by *Haagen-Smit et al.* [1953], while methane and carbon monoxide (CO) are thought to be important only on the global scale due to their relatively low reactivities [*Chameides et al.*, 1992]. The dependence of the daily ozone maximum on early morning concentrations of precursors NOx and NMOC has been recognized for many years [*Seinfeld*, 1989; *Committee on Tropospheric Ozone Formation and Measurement*, 1991; *Seinfeld and Pandis*, 1998; *Jacobson*, 2002]. It is generally thought that ozone formation is NOx sensitive when the NMOC/NOx ratio is over 8:1 and NMOC sensitive when this ratio is less than 8:1, although actual conditions rely on many other factors. Under low NMOC/NOx ratios, early morning NMOC composition is particularly important [*Committee on Tropospheric Ozone Formation and Measurement*, 1991; *Sillman*, 1999]. This work is focused on investigating morning NMOC/NOx ratios as well as NMOC composition to examine ozone forming sensitivity in urban Shanghai.

[4] NMOCs exhibit a wide range of reactivities with respect to ozone photochemical formation. Several reactivity scales have been introduced to avoid a misleading view that can arise from the measured concentrations, and to scale the relative ozone forming capacity of different NMOC species [*Dodge*, 1984; *Atkinson*, 1990; *Middleton et al.*, 1990; *Carter*, 1994; *DeMore et al.*, 1997]. A widely used scaling method is Incremental Reactivity (IR) defined as the amount of ozone formed per unit of NMOC added or subtracted from the whole mixture in a given air mass, which is comprised of the kinetic and mechanistic reactivities [*Atkinson*, 2000]. The Maximum Incremental Reactivity (MIR) factors were developed by *Carter* [1994] in model scenarios, under which NOx has the strongest ozone inhibiting effect representing a typical NMOC-limited condition. Photochemical Ozone Creation Potentials (POCP) are also useful in assessing ozone forming potentials of different species and have been calculated with a master chemical mechanism over northwest Europe [*Derwent et al.*, 1998]. Another widely used scale is the OH-reactivity scale which is based on an assumption that mechanistic differences among NMOC species are comparatively small in comparison to the kinetic differences [*Darnall et al.*, 1976; *Middleton et al.*, 1990; *Atkinson*, 1990; *Chameides et al.*, 1992; *DeMore et al.*, 1997]. Hence NMOC reactivity is scaled by weighting various NMOC species with their OH radical reaction rate constants. The MIR and OH-reactivity ranking methods each have advantages and disadvantages [*Dimitriades*, 1996]. The MIR method takes into consideration the chemical mechanisms and impacts of NMOC/NOx ratios on ozone production, but has chemical mechanism and simulation uncertainties. The OH reactivity method relies on assumptions that reaction with OH radical is dominant and that the mechanistic factor and its associated uncertainties are negligible. Consequently both of these factors are considered in the following NMOC analysis.

[5] Although we focus on ozone precursor relationships of the local photochemical processes under transport-limited conditions, it should be noted that other influencing factors of comparable importance exist. These factors include radiation, heterogeneous reactions, deposition and entrainment and they cannot be characterized by analyzing ground level measurements [*Trainer et al.*, 2000]. Model simulations are required to investigate these processes. Effects of clouds and aerosols on radiation flux and ozone photochemical production have been investigated in previous studies [*Bian et al.*, 2007; *Zhang et al.*, 2007]. Issues concerning aerosol impacts on radiation and ozone will be covered in this paper.

2. Data and Methods

2.1. Measurements

[6] Measurements of ground level ozone, NOx, CO and NMOC concentrations were performed nearly every day between 15 June 2006 and 14 June 2007 at an urban site (31°12′N, 121°26′E) in Shanghai. The monitoring location is within a populated urban area with busy traffic and numerous tall buildings. A large petrochemical complex in the Jinshan District is about 50 km to the south of the monitoring site.

[7] Ozone, NOx and CO were measured with a one minute averaging time using calibrated instruments installed on top of a 15 meter high building, and were reported as volume mixing ratios (ppbv). A UV absorption ozone analyzer (EC9810B/ECOTECH) that meets the technical requirements of the USEPA was used to measure ambient ozone concentrations. The oxides of nitrogen analyzer (EC9841B/ECOTECH) had a heated molybdenum NO_2 to NO converter. The resulting NO concentration was quantified using the chemiluminescence technique. CO was observed using an EC9830B/ECOTECH carbon monoxide analyzer. NMOCs were collected using 6 L canisters using EPA method TO 15 for the 24-hour and morning (6:00–9:00 a.m.) sampling periods. A total of 109 individual species were identified and mixing ratios reported in ppbv (Table 1). The detailed analytical method for NMOC species can be found somewhere else [*Geng et al.*, 2006]. Meteorological data including wind, temperature, cloud amount, and the past 6-hour precipitation total were obtained every three hours beginning at 2:00 a.m. from a local meteorological station. The 550 nm aerosol optical depth (AOD) data used for this study were Level 2 aerosol products provided by Moderate Resolution Imaging Spectroradiometer (MODIS) on NASA's Terra and Aqua spacecrafts with a spatial resolution of 10 km.

2.2. Data Analysis

[8] One-minute average ozone, NOx and CO data were used to calculate 1-hour averages when the missing data comprised less than 25% of the total. Other cases were considered as missing data for that hour. The 109 NMOC target species were represented using three approaches. The first approach was to express the measurements as carbon atom-based concentrations (ppbC). The second involved weighting each species by its OH reactivity and normalizing this value relative to the equivalent reactivity for propene [*Committee on Tropospheric Ozone Formation and Measurement*, 1991; *Chameides et al.*, 1992]. The resulting Propy-Equiv concentration is thus calculated by multiplication of ppbC concentration and the relevant OH reaction rate constant (obtained primarily from *Atkinson* [1990], also

Table 1. Properties of 24-Hour Integrated NMOC and 6:00–9:00 a.m. NMOC at an Urban Site in Shanghai

				24-Hour Integrated Averages (ppbC)		6:00–9:00 a.m. Averages (ppbC)	
	Species	$k_{OH} \times 10^{12}$[a]	MIR[b]	Mean	Std. Dev.	Mean	Std. Dev.
			Alkanes				
1	ethane	0.24	0.25	2.20	5.45	6.76	53.45
2	propane	1.1	0.48	12.76	6.75	14.64	10.07
3	isobutane	2.34	1.21	3.87	3.41	5.19	5.07
4	butane	2.54	1.02	7.19	3.81	8.66	6.43
5	isopentane	3.9	1.38	9.88	6.04	12.11	10.27
6	*n*-pentane	3.94	1.04	6.98	7.04	8.10	8.33
7	2,2-dimethylbutane			0.00	0.00	0.00	0.00
8	cyclopentane	5.16	2.4	1.55	1.83	1.51	1.90
9	2,3-dimethylbutane	6.3	1.07	3.13	2.67	2.98	2.79
10	2-methylpentane	5.6	1.5	3.76	3.27	4.36	5.18
11	3-methylpentane	5.7	1.5	2.43	2.96	2.88	4.87
12	*n*-hexane	5.61	0.98	4.50	4.81	5.01	7.60
13	2,4-dimethylpentane	5.1	1.5	1.00	1.25	1.28	1.94
14	methylcyclopentane	7.05	2.8	0.57	1.12	0.79	1.84
15	cyclohexane	7.49	1.28	0.19	0.71	0.29	0.80
16	2-methylhexane	7.18	1.08	0.70	1.23	0.93	1.64
17	2,3-dimethylpentane		1.31	0.21	0.74	0.33	0.87
18	3-methylhexane	7.18	1.40	0.70	1.41	0.97	1.90
19	2,2,4-trimethylpentane	3.68	0.93	2.27	3.29	2.22	2.66
20	*n*-heptane	7.15	0.81	0.57	1.20	0.83	1.67
21	methylcyclohexane	10.4	1.8	0.06	0.29	0.19	0.59
22	2,3,4-trimethylpentane	7	1.6	0.00	0.00	0.01	0.19
23	2-methylheptane		0.96	0.01	0.13	0.06	0.32
24	3-methylheptane	8.54	0.99	0.02	0.20	0.14	0.59
25	*n*-octane	8.68	0.60	0.06	0.32	0.16	0.60
26	nonane	10.2	0.54	0.16	0.70	0.26	0.89
27	*n*-decane	11.6	0.46	0.30	1.13	0.51	1.58
28	*n*-dodecane	14.2	0.38	0.17	1.04	0.28	1.65
29	*n*-undecane	13.2	0.42	0.21	0.80	0.33	1.13
			Alkenes				
1	propene	26.3	9.4	2.79	3.20	3.70	6.18
2	1-butene	31.4	8.9	2.44	2.11	2.87	2.47
3	1,3-butadiene	66.6	10.9	0.06	0.75	0.07	0.56
4	*cis*-2-butene	56.4	10.0	0.10	0.53	0.43	1.58
5	*trans*-2-butene	64	10.0	0.16	0.72	0.52	1.88
6	2-methyl-2-butene	68.9	6.4	0.00	0.00	0.00	0.00
7	1-pentene	31.4	6.2	0.01	0.13	0.12	0.62
8	isoprene	101	9.1	0.17	0.51	0.38	1.18
9	*cis*-2-pentene	65	8.8	0.28	0.68	0.48	1.06
10	*trans*-2-pentene	67	8.8	0.27	0.68	0.50	1.14
11	cyclopentene	67	7.7	0.00	0.00	0.00	0.00
12	4-methyl-1-pentene			0.01	0.17	0.01	0.13
13	*cis*-2-hexene	62.7	6.7	0.00	0.00	0.00	0.00
14	*trans*-2-hexene	62.6	6.7	0.00	0.00	0.00	0.00
15	acetylene	0.83	0.5	7.15	5.45	8.14	7.94
			Aromatics				
1	styrene	10.0	2.2	0.68	1.14	0.84	1.94
2	benzene	1.23	0.42	10.04	6.07	11.67	9.57
3	toluene	5.96	2.7	32.81	21.61	36.13	36.72
4	ethylbenzene	7.1	2.7	12.04	7.53	10.90	10.11
5	m-xylene	23.6	8.2	6.85	5.00	6.85	7.20
6	*p*-xylene	14.3	6.6	3.65	2.59	3.86	3.87
7	*o*-xylene	13.7	6.5	8.36	16.02	9.67	24.42
8	isopropylbenzene	6.5	2.2	0.34	0.81	0.46	1.71
9	*n*-propylbenzene	6.0	2.1	0.29	0.58	0.38	0.82
10	1,3,5-trimethylbenzene	57.5	10.1	1.57	1.02	1.33	1.05
11	1,2,4-trimethylbenzene	32.5	8.8	1.56	1.26	1.73	1.76
12	*m*-ethyltoluene	19.2		1.57	1.53	1.63	1.98
13	*p*-ethyltoluene	12.1		1.15	0.71	1.03	0.84
14	*o*-ethyltoluene	12.3		0.14	0.36	0.25	0.76
15	*m*-diethylbenzene	24.3		0.08	0.39	0.22	0.77
16	*p*-diethylbenzene			0.09	0.42	0.23	0.83
17	1,2,3-trimethylbenzene	32.7	8.9	0.12	0.38	0.22	0.62

Table 1. (continued)

	Species	$k_{OH} \times 10^{12}$[a]	MIR[b]	24-Hour Integrated Averages (ppbC) Mean	24-Hour Integrated Averages (ppbC) Std. Dev.	6:00–9:00 a.m. Averages (ppbC) Mean	6:00–9:00 a.m. Averages (ppbC) Std. Dev.
			Halogenated alkanes				
1	dichlorodifluoromethane	0.000006		0.58	0.15	0.59	0.16
2	chloromethane	0.036		1.04	1.51	1.31	2.70
3	freon-114			0.00	0.00	0.00	0.00
4	bromomethane	0.029		0.00	0.00	0.00	0.00
5	chloroethane	0.407		0.00	0.00	0.01	0.12
6	trichlorofluoromethane	0.000005		0.31	0.20	0.30	0.14
7	trichloro-trifluoroethane			0.00	0.02	0.01	0.07
8	dichloromethane	0.11		0.87	0.94	0.72	0.86
9	1,1-dichloroethane			0.02	0.10	0.05	0.27
10	chloroform	0.1		0.07	0.15	0.10	0.23
11	1,1,1-tricholoethane			0.00	0.02	0.00	0.00
12	1,2-dichloroethane			2.68	3.13	3.09	4.96
13	carbon tetrachloride	0.0005		0.05	0.13	0.06	0.17
14	1,2-dichloropropane			0.13	0.67	0.32	1.56
15	bromodichloromethane			0.00	0.00	0.00	0.00
16	1,1,2-trichloroethane			0.00	0.00	0.003	0.03
17	dibromochloromethane			0.001	0.02	0.004	0.03
18	1,2-dibromoethane			0.00	0.00	0.00	0.00
19	bromoform	0.15		0.00	0.00	0.00	0.00
20	1,1,2,2-tetrachloroethane			0.00	0.00	0.00	0.00
			Halogenated alkenes				
1	vinyl chloride	6.57		1.30	3.82	1.99	6.50
2	vinyl bromide			0.00	0.00	0.00	0.00
3	1,1-dichloroethene			0.00	0.00	0.01	0.13
4	allyl chloride			0.00	0.00	0.00	0.00
5	*trans*-1,2-dichloroethylene	2.3		0.00	0.00	0.00	0.00
6	*cis*-1,2-dichloroethylene	2.3		0.00	0.03	0.00	0.00
7	trichloroethylene	2.2		0.04	0.17	0.10	0.45
8	*cis*-1,3-dichloropropene			0.00	0.00	0.00	0.00
9	*trans*-1,3-dichloropropene			0.00	0.06	0.05	0.25
10	tetrachloroethylene	0.17		0.04	0.12	0.06	0.15
11	hexachloro-1,3-butadiene			0.00	0.00	0.00	0.00
			Halogenated aromatics				
1	chlorobenzene	0.949		0.13	0.34	0.26	0.56
2	1,3-dichlorobenzene			0.61	0.75	0.92	1.06
3	benzyl chloride			0.00	0.00	0.00	0.00
4	1,4-dichlorobenzene	0.339		0.62	0.76	0.92	1.06
5	1,2-dichlorobenzene			0.01	0.12	0.09	0.43
6	1,2,4-trichlorobenzene			0.01	0.15	0.00	0.00
			Oxygenated hydrocarbons				
1	isopropyl alcohol	5.21	0.54	0.11	0.67	0.60	3.54
2	propanal	19.6	6.5	0.00	0.00	0.00	0.00
3	tetrahydrofuran			0.02	0.14	0.09	0.46
4	1,4-dioxane			0.00	0.00	0.00	0.00
5	vinyl acetate			0.12	0.43	0.23	0.81
6	ethyl acetate	1.69		7.08	6.89	7.62	10.49
7	acetone	0.22	0.56	4.54	8.12	5.69	11.08
8	2-butanone	1.15	1.18	5.12	4.98	5.77	7.44
9	methyl isobutyl ketone	14.1		0.05	0.32	0.20	0.72
10	2-hexanone	9.1		0.01	0.17	0.18	3.22
11	methyl *tert*-butyl ether	2.83	0.62	0.77	1.39	1.26	2.19
Total				186.56	116.11	218.96	190.08
CO		0.24		823	403	933	590

[a]OH radical reaction rate constant at $T = 298$K in the unit of cm^3 $molecule^{-1}$ s^{-1}.
[b]Maximum incremental reactivity (MIR) factor in the unit of g O_3/g NMOCs.

from *Middleton et al.* [1990] and *DeMore et al.* [1997]) normalized to that of propene. The final approach, referred to here as MIR factors (g Ozone/g NMOCs), is based on the approach developed by *Carter* [1994]. NMOCs were classified into five categories: alkanes, alkenes (including acetylene), aromatics, oxygenated hydrocarbons (including aldehydes, ketones, alcohols, ethers and esters) and halocarbons (including halogenated alkanes, alkenes and aromatics).

2.3. Model Description

[9] Two models were used for this study. The first model, OZIPR, is a trajectory-type air quality simulation model with user controlled specific input files [*Gery and Crouse*, 1990]. The model simulates complex chemical reactions within a well-mixed column of air extending from the ground to the top of the mixed layer as it moves with wind.

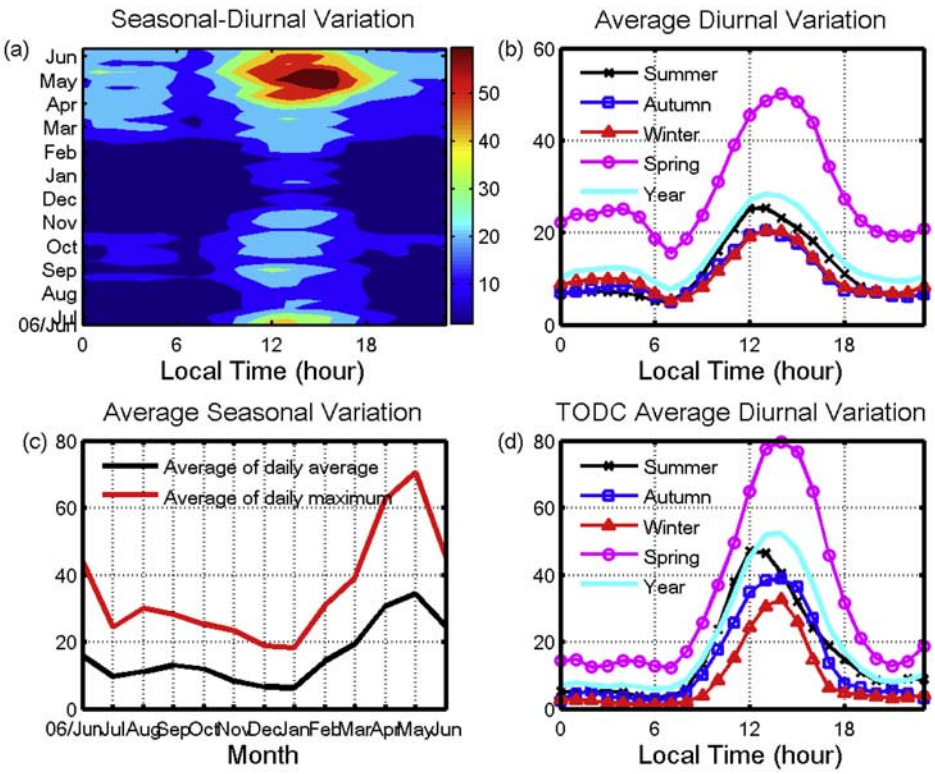

Figure 1. Ozone observations (ppbv) in downtown of Shanghai from summer 2006 to spring 2007. (a) Seasonal-diurnal variations with daily 1-hour averages and days of each month averaged into three parts. (b) Average diurnal patterns of each season and the whole year. (c) Monthly mean of daily average and daily maximum. (d) Average diurnal patterns of TODC days (defined as "typical ozone diurnal cycle" in section 3.2) for each season and for the year.

Ozone precursor concentrations and ambient information such as temperature, relative humidity and boundary layer height can be specified for each single run. Therefore a series of simulations can be performed to calculate ozone levels as a function of initial precursor concentrations.

[10] The second model used for this study was the NCAR Master Mechanism (NCAR-MM) model, which is a photochemical box model with detailed gas phase chemical mechanism containing nearly 5000 reactions [*Madronich and Calvert*, 1990; *Herring et al.*, 1997]. This model simulates the chemical time evolution of an air parcel initialized with user defined input parameters, including constrained species concentrations, emissions, temperature, dilution and boundary layer height. The photolysis rates are calculated with the Tropospheric Ultraviolet and Visible Radiation (TUV) model [*Madronich and Flocke*, 1998] under user specified conditions such as location, time, elevation, and optical depth of cloud and aerosol.

3. Results and Discussion

3.1. Characteristics of Ozone, NOx, CO, and NMOCs

3.1.1. Ozone

[11] Seasonal and diurnal characteristics of ozone observations are displayed in Figures 1a–1c. During the observation period, spring was the most productive season for ozone with the highest daily maximum (128 ppbv) occurring in May. This peculiar trait of peaking in spring instead of summer may be explained by the ozone-inhibiting influence of the rainy season (Meiyu period) during summertime in the Yangtze River area of China. A more detailed explanation will require a longer observation sequence of ozone and its precursors to quantify the relative role of meteorology and chemistry. The average diurnal cycle shows a single daily maximum after noon, and reflects the important contributions of photochemistry. The minimum in the early morning may result from high NO emission due to transportation during rush hour periods. Monthly means of daily averages range from 6 to 28 ppbv during the observation period with lower concentrations in winter. Monthly averages of daily maximums show a similar seasonal variation, ranging from 17 to 70 ppbv.

3.1.2. NOx

[12] Measured NOx reaches a maximum in winter and a minimum in summer due to a combination of processes (Figures 2a and 2c). High levels of NOx in winter could result from lower removal rates due to lower reaction rates at lower temperatures, lower OH concentrations due to lower actinic flux, and lower vertical dispersion due to a shallower boundary layer. In summer, NOx is removed much faster due to higher reaction rates [*Jacobson*, 2002; *Seinfeld and Pandis*, 1998]. The diurnal NOx cycle displays a typical double peak, representing heavy traffic in the morning and evening rush hour periods (Figure 2b). The daily average NOx was about 50 ppbv, with higher levels in winter and lower levels in summer. For 6:00–9:00 a.m. rush hours, yearly average NOx reached about 60 ppbv with a range of 12 to 400 ppbv.

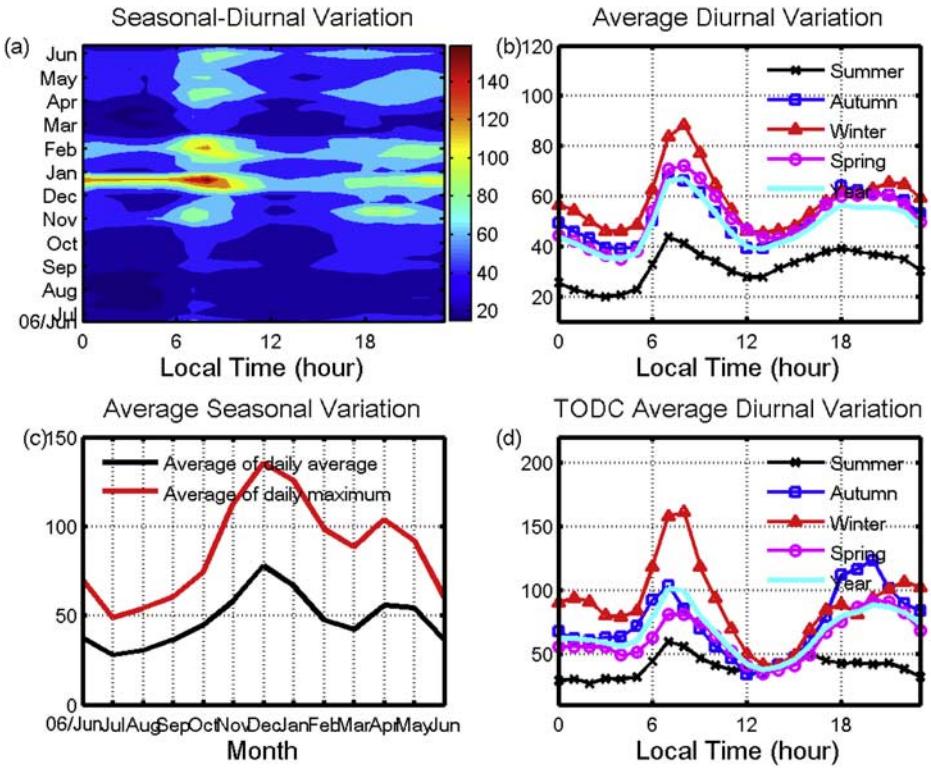

Figure 2. NOx observations displayed as in Figure 1.

[13] The use of a Mo converter has important implications for interpreting these data. Many papers have addressed issues associated with NOx converters and have compared conventional surface conversion techniques with new techniques such as photolytic conversion and laser induced fluorescence [e.g., *Fehsenfeld et al.*, 1990; *Committee on Tropospheric Ozone Formation and Measurement*, 1991; *Chameides et al.*, 1992; *Parrish and Fehsenfeld*, 2000; *Steinbacher et al.*, 2007]. Due to the interference of other reactive nitrogen compounds, NOx can be overestimated when using surface converters, especially in rural/remote areas and aged plumes. However, the Mo converter is considered to be a reasonable technique for characterizing NOx in freshly polluted urban air.

3.1.3. CO

[14] CO exhibits a temporal pattern similar to NOx. Figures 3a–3c shows that CO also displays a double-peak diurnal cycle and a seasonal variation that peaks in winter. The similarity between CO and NOx may be explained by their common sources including vehicular exhaust in urban areas and because they have similar chemical losses controlling their temporal patterns. The apparent double peak suggests that motor vehicles are the main source of CO in urban Shanghai, even though CO possesses a long lifetime and could be transported from other regions. Daily average CO levels are 823 ppbv, ranging from 200 to 3500 ppbv. For the early morning rush hours, CO averages 932 ppbv with a range of 122 to 5010 ppbv.

3.1.4. NMOCs

[15] The temporal patterns of total NMOC for the morning and the 24-hour sampling periods are similar and display large day-to-day variations (Figure 4). Morning ambient concentrations generally exceed that of the 24-hour integrated samples, implying emissions in rush hours are one of the major sources of the 24-hour period. Average total NMOC concentrations range from 30 to 784 ppbC for daily sampling and from 22 to 1536 ppbC for morning sampling, showing a larger variability for morning. There does not appear to be a seasonal cycle (Figure 4). This particular feature may be associated with the prevailing southerly summer wind over the Shanghai region, which brings pollutants such as halogenated NMOC and aromatics from petrochemical facilities in Jinshan. Both photochemistry and the combined sources probably result in a seasonal pattern of NMOC that is quite different from that of NOx and CO, which are mainly of vehicular origin and exhibit a significant seasonal cycle. It is interesting to note that a period of reduced total NOMC concentrations lasts for almost a month from mid February to mid March, which also was observed for NOx and CO. Sharply reduced emissions from automobiles and factories during the traditional Spring Festival in China (in the year 2007, beginning from 18 February and lasting for almost one month) likely accounts for this phenomenon.

[16] Four metrics were used to obtain an overall understanding of NMOC composition. As illustrated in Figure 5, daily and morning samples have almost no difference in composition for all metrics. For the volume mixing ratio metric, alkanes account for nearly 40% of the total mixture, followed by aromatics with about 25%. Alkenes, oxygenated hydrocarbons and halocarbons are comparable. The alkanes are dominated by light alkanes with less than five carbon atoms, which are thought to come largely from vehicular exhaust and evaporation according to the USEPA (2002). Aromatics and alkanes are equivalent, with a fraction of about 40%, when expressed as carbon atom

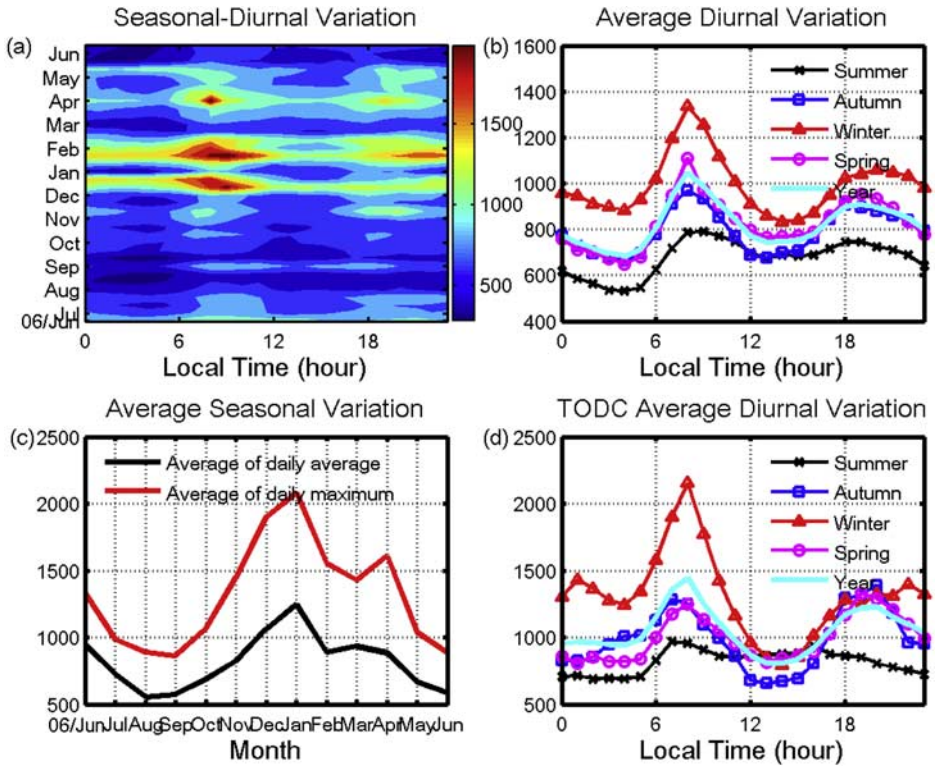

Figure 3. CO observations displayed as in Figure 1.

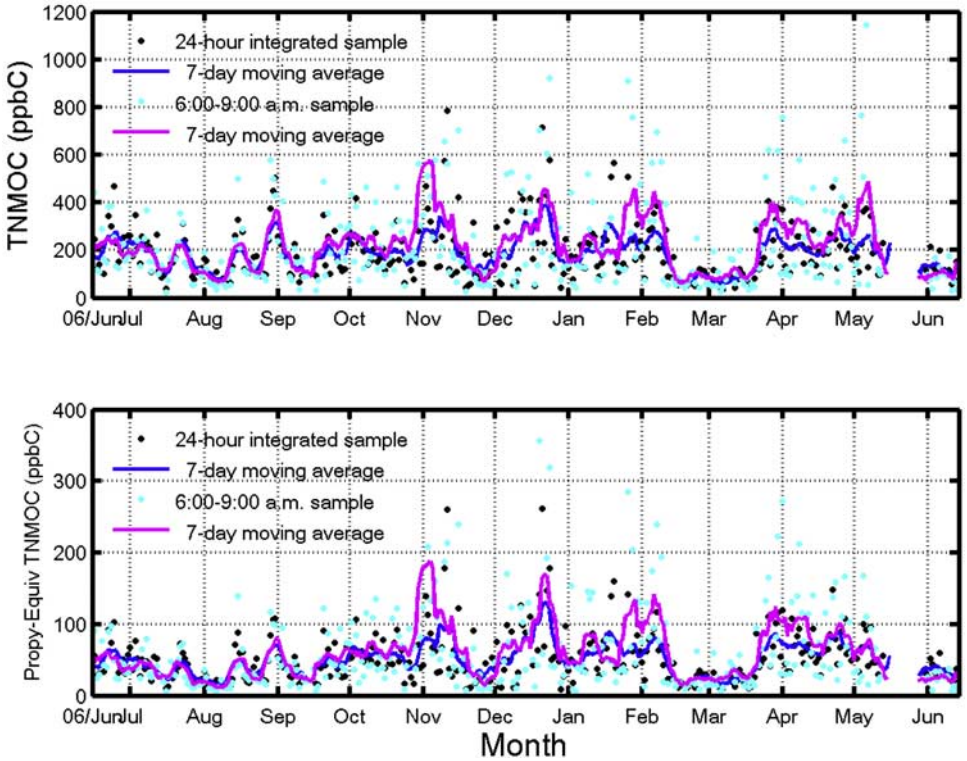

Figure 4. NMOC observations in downtown of Shanghai during summer 2006 to spring 2007. Dots represent daily observed value, lines represent 7-day moving average. (top) Total NMOC concentrations from 24-hour integrated sampling and morning (6:00–9:00 a.m.) sampling; (bottom) total Propy-Equiv NMOCs concentrations of both 24-hour and morning sampling periods.

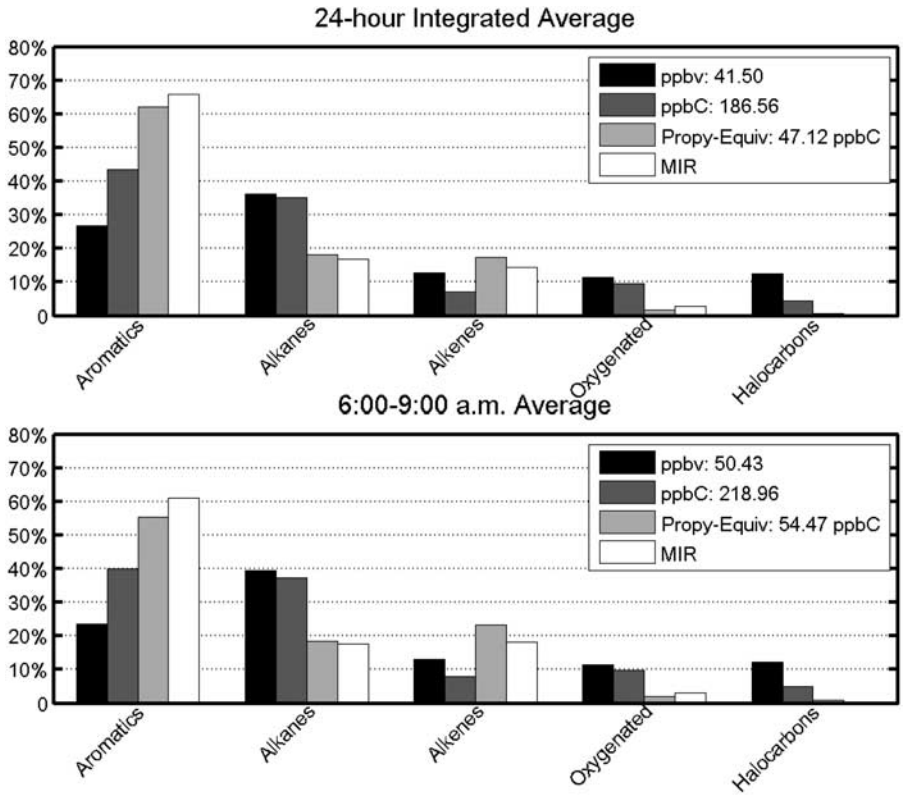

Figure 5. Average fractions of each category based on volume mixing ratio (ppbv), carbon-atom-based concentration (ppbC), OH-reactivity-based Propy-Equiv concentration (ppbC), and MIR factor weighted fraction. Halocarbons are not included in MIR values due to lack of MIR factors. The average ppbv, ppbC, and Propy-Equiv concentrations are also given at the top of the diagram: (top) for 24-hour integrated averages and (bottom) for 6:00–9:00 a.m. averages.

mixing ratios. This demonstrates an overemphasis of the importance of light alkanes expressed as ppbv. The calculated total Propy-Equiv mixing ratio is about one quarter of the ambient ppbC concentration. This implies that the major NMOC components in urban Shanghai are less reactive than propene. Whereas aromatics are comparable to alkanes by carbon atom based mixing ratio, the OH-reactivity and MIR scale all reveal that aromatics play a dominant role in contributing to total NMOC reactivity and ozone formation potential. The contribution of CO to total reactivity (CO and NMOC) is calculated to be about 13%. Consistent with the conclusions of *Chameides et al.* [1992], it is NMOC rather than CO that serve as the major ozone precursor in an urban area.

[17] Comparisons of NMOC composition between different cities were conducted on the basis of fractional contribution using ppbC units. A summary of NMOC composition in twelve urban locations and two industrial areas is provided in Figure 6, although absolute results may depend on selected species as well as sampling time and duration. NMOC composition varies greatly between different cities. Higher alkene fractions are found in heavily industrialized cities with oil refineries and petrochemical facilities, such as Houston and Ulsan. Two composition patterns are generally found with aromatics or alkanes dominating. On average, the NMOC composition in Shanghai is similar to cities with higher aromatic levels like Kaohsiung, Osaka and Hamburg. Nonetheless, it should be borne in mind that similar NMOC composition does not necessarily result from similar emission patterns. Specific measurements and analyses are required to gain further insight into source apportionment. Furthermore, it is also important to note that it is difficult to categorize cities, particularly in the case of rapidly developing megacities like Shanghai.

[18] The seasonal variation of NMOC composition was examined with the ppbC mixing ratio. Aromatics and alkanes were found to be major components with aromatics slightly exceeding alkanes for both types of averages (Figures 7a and 7c). In autumn and spring, aromatics increased to nearly 50%, greater than alkanes at 30%, in contrast to other seasons when alkanes dominate over aromatics or both are about equal at 40%. A change in the fractions of alkanes and aromatics would lead to a change in total NMOC reactivity and thus the ozone formation processes. In Figures 7b and 7d, it can be seen that aromatics dominate the total NMOC reactivity and ozone forming potential throughout the period.

[19] For individual species, we find that the top 10 species of both samples are the same for OH-reactivity ranking and MIR ranking, with only a slight difference in their order (Table 2). The MIR top 10 species contribute nearly 80% of the ozone production potential and are mainly composed of aromatic species. Toluene and xylene are important in urban Shanghai whether based on ppbC mixing ratios or ozone production potential. Their major

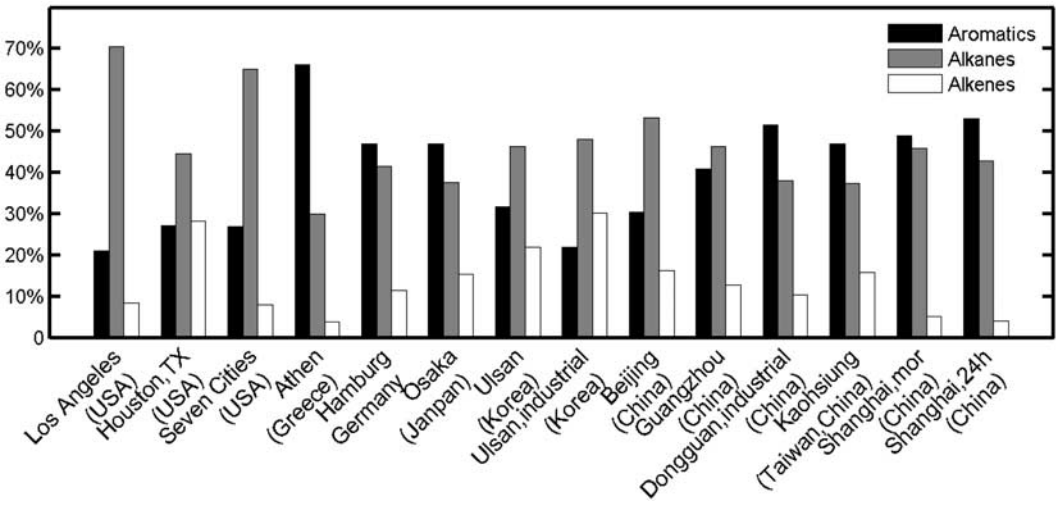

Figure 6. Fractions of NMOC categories in various cities. For the sake of consistency, acetylene is not included in alkenes: Los Angeles, Houston, Texas [*Baker et al.*, 2008]; Seven Cities (calculated average results of seven cities from *Sexton and Westberg* [1984]); Hamburg, Athens, Osaka [*Moschonas and Glavas*, 1996]; Ulsan [*Na et al.*, 2001]; Beijing [*Duan et al.*, 2008]; Guangzhou, Dongguan [*Barletta et al.*, 2008]; Kaohsiung in southern Taiwan [*Chang et al.*, 2005]; Shanghai (this paper).

sources are vehicular exhaust and petrochemical industries [*Qian and Zhang*, 1999; *Na et al.*, 2001; *EPA*, 2002]. It is noteworthy that vinyl chloride, a hazardous air pollutant thought to be mostly emitted from petrochemical industries [*Na et al.*, 2001], has a considerable amount of 0.65 ppbv for daily average and 1.0 ppbv averaged over the morning period, and is especially abundant in summertime. It implies that industrial emissions in Jinshan may be responsible for a portion of the background NMOCs in this urban area. The present vegetation coverage in Shanghai contributes to isoprene being the major NMOC with biogenic sources, although it should be noted that vehicular emissions are also

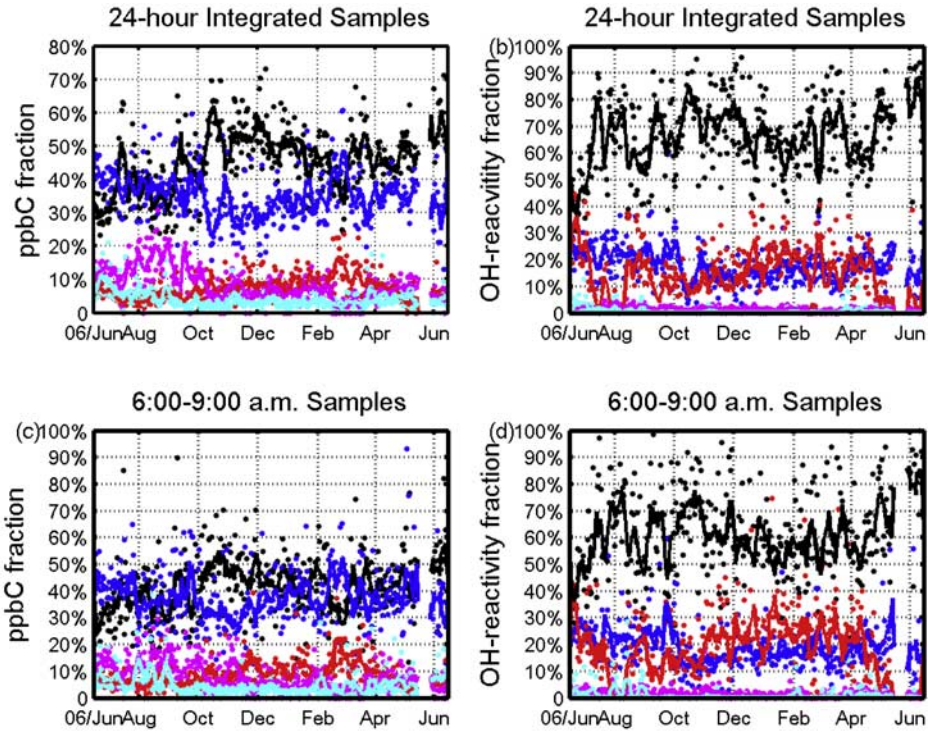

Figure 7. Fractions of each category for two scales: carbon-atom-based concentration and OH-reactivity-based concentration. Dots represent daily values; lines represent 7-day moving average. The five categories are aromatics (black), alkanes (blue), alkenes (red), oxygenated hydrocarbons (magenta), and halogenated hydrocarbons (cyan).

Table 2. Top 10 Species by OH Reactivity Ranking and MIR Ranking

	24-Hour Integrated Averages					6:00–9:00 a.m. Averages			
	OH Reactivity Ranking		MIR Ranking			OH Reactivity Ranking		MIR Ranking	
Number[a]	Species	%	Species	%	Number	Species	%	Species	%
1	toluene	14.7	toluene	19.7	1	toluene	13.7	toluene	19.0
11	*m*-xylene	12.1	*m*-xylene	12.6	11	*m*-xylene	10.3	*o*-xylene	12.3
6	*o*-xylene	8.6	*o*-xylene	12.2	6	*o*-xylene	8.4	*m*-xylene	11.0
26	1, 3, 5-trimethylbenzene	6.8	ethylbenzene	7.3	19	propene	6.2	propene	7.2
3	ethylbenzene	6.4	propene	6.2	22	1-butene	5.7	ethylbenzene	5.7
21	1-butene	5.7	p-xylene	5.4	5	ethylbenzene	4.9	1-butene	5.3
19	propene	5.5	1-butene	5.1	29	1, 3, 5-trimethylbenzene	4.8	p-xylene	5.0
17	p-xylene	3.9	1, 3, 5-trimethylbenzene	3.5	26	1, 2, 4-trimethylbenzene	3.6	isopentane	3.5
27	1, 2, 4-trimethylbenzene	3.8	isopentane	3.3	18	p-xylene	3.5	1, 2, 4-trimethylbenzene	3.0
5	isopentane	2.9	1, 2, 4-trimethylbenzene	3.0	3	isopentane	3.0	1, 3, 5-trimethylbenzene	2.6

[a]Number gives the ppbC concentration ranking.

an isoprene source. Isoprene is ranked below the 50th and 25th position for the ppbC and MIR method, respectively. Thus NMOCs mostly come from anthropogenic sources rather than biogenic sources in urban Shanghai. According to *Bell and Ellis* [2004], biogenic NMOCs can exert a considerable impact on ozone formation. Considering such important effects combined with the comparatively high rank of biogenic NMOC reactivity, ozone increases in urban Shanghai may occur if biogenic emissions continue to increase with more vegetation cover.

[20] The temporal variation of fractions of aromatics and alkanes suggests various sources contributing to NMOCs in urban Shanghai [*Bottenheim et al.*, 1997; *Chang et al.*, 2005; *Na*, 2006]. The vehicular exhaust indicator, methyl tert-butyl ether, has been used to find which NMOC are primarily related to traffic emissions [*Chang et al.*, 2003]. However, correlations between primary exhaust components and the indicator are generally poor. Lack of correlation implies that traffic emission is not the only important source of NMOCs in urban Shanghai. Considerable contributions must come from other sources. In urban areas, evaporation of solvents and paint from tall buildings is a notable NMOC source. Petrochemical industries about 50 km south of Shanghai provide elevated background concentrations of certain NMOC species such as aromatics, heavy alkanes [*Qian and Zhang*, 1999] and halocarbons. Also, the policy of high license plate taxes for private cars has effectively limited the number of automobiles in Shanghai and helps reduce the contribution of traffic emissions.

3.2. Relationships of Ozone, Nox, and NMOCs

[21] Ozone precursor relationships are crucial for understanding local ozone photochemical processes. Assessing whether an area is NOx-limited or NMOC-limited is an important step for developing effective ozone control strategies. A method based on field observations of ambient ozone precursor concentrations could be exploited for investigating this issue. NMOC/NOx ratios in the early morning are typically used for this purpose. Figure 8 (bottom) shows that about 91% of all the early morning NMOC/NOx ratios

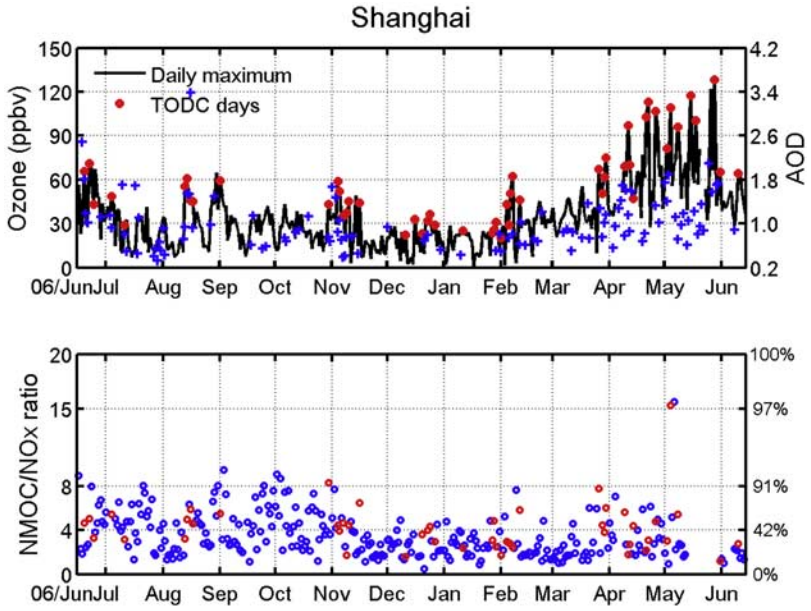

Figure 8. (top) Daily 1-hour average ozone maximum concentrations (black line) and MODIS AOD data (blue crosses). Values on TODC days are marked with red dots. (bottom) NMOC (ppmC)/NOx (ppmv) ratios, percentage of ratios below a certain value is shown on the right. Values on TODC days are marked with red circles.

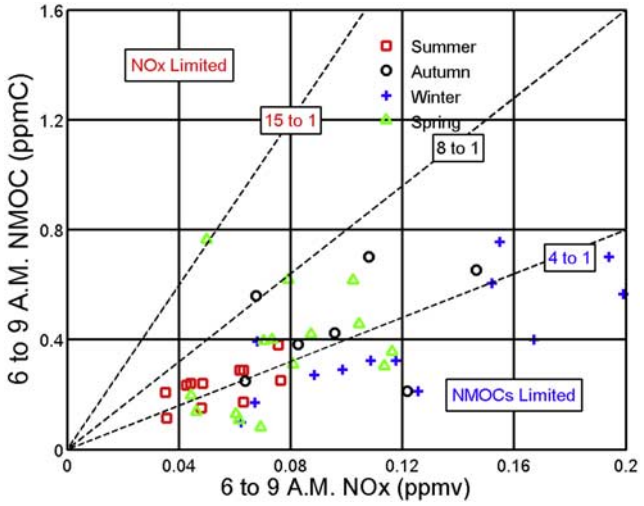

Figure 9. NMOC/NOx ratios on TODC days in downtown Shanghai during summer 2006 to spring 2007. Four TODC days with missing NMOC or NOx data are not shown. Two points with large NOx concentrations are also not shown: NOx = 2.86 ppmv, NMOC/NOx = 2.44; NOx = 2.11 ppmv, NMOC/NOx = 4.36.

are less than 8 and about half are below 4. The ratio distribution shows that moderate early morning NMOC/NOx ratios are the typical case in urban Shanghai.

[22] Since the empirical method is valid only if there is limited transport, it is not reasonable to apply this method to the entire period of observation. Therefore we selected cloudless days without precipitation during the day and with a wind speed of less than 4 m/s. Under such circumstances, transport, wet deposition and radiation reduction due to cloud effects were considered negligible. Average diurnal variations of ozone, NOx and CO are shown in Figures 1d–3d. On these days, ozone displays a sinusoidal curve with a single daily maximum after noon, which is referred to here as the typical ozone diurnal cycle (TODC). With these constraints, we obtained a data set of 52 TODC days, for which the peak ozone values are shown in Figure 8 with red dots. Hence TODC days mainly reflect local photochemical ozone formation even though there may be other contributing processes. For such photochemistry dominated cases, early morning NMOC/NOx ratios are considered to be the most relevant for ozone precursor relationship analysis. Nearly all TODC NMOC/NOx ratios are situated in the NMOC-limited region and center around the 4:1 ratio line (Figure 9). This indicates the NMOC sensitivity of ozone photochemical formation at this location. Since the separation between NOx-limited and NMOC-limited regions relies on many factors, especially the early morning NMOC composition under low NMOC/NOx ratios, a further exploration of NMOC composition was conducted. Similar to early morning NMOC composition of the entire period, NMOCs during TODC periods exhibit a low Propy-Equiv mixing ratio which suggests a relatively low reactivity.

[23] To investigate ozone precursor relationships, a series of simulations were also performed using OZIPR. A base case was obtained by using average measured ground level concentrations of early morning NOx, CO, NMOC and local meteorological data. The NOx and NMOC levels were then modified to simulate different cases. Figure 10 illustrates the simulation results for 225 runs and shows the base case as a black dot. The sensitivity to precursors is quite different for each regime. The regime near the base case demonstrates a behavior of declining ozone with increasing NOx and decreasing NMOC. The simulation result supports our conclusion that urban Shanghai is typically NMOC-limited. In the future, an increase in automobiles in Shanghai will increase NMOC and NOx concentrations and change the morning NMOC/NOx ratios, overall NMOC composition and reactivity. Figure 10 shows that this can result in either higher or lower ozone, depending on whether NOx or NMOCs increase more.

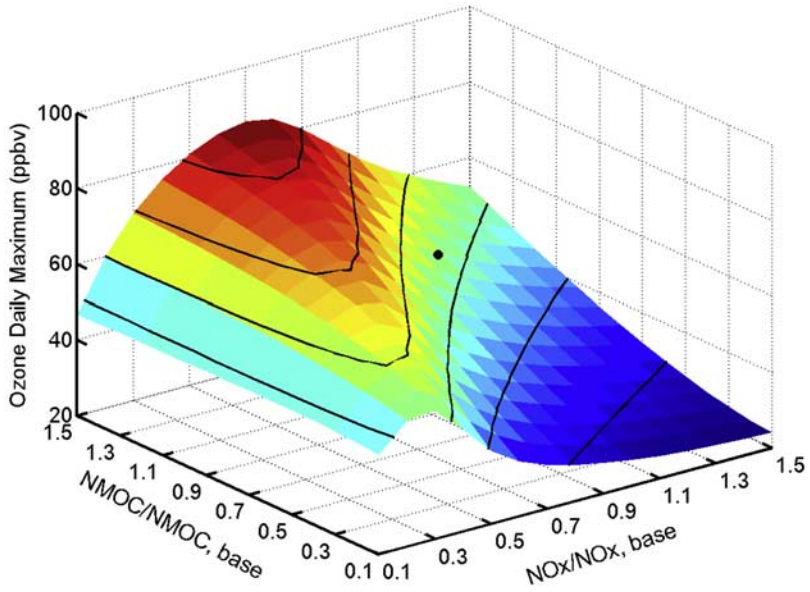

Figure 10. Daily ozone maxima calculated from different initial NOx and NMOC concentrations. NOx, base = 93 ppbv; NMOC, base = 0.315 ppbC. Base case with ozone = 57.6 ppbv is marked by a black dot.

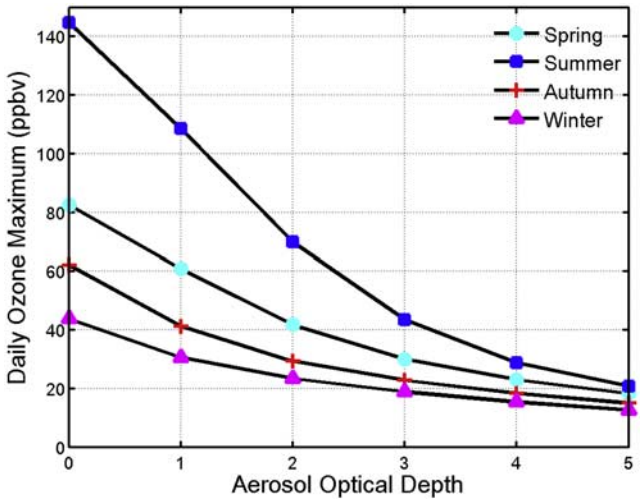

Figure 11. NCAR-MM model simulation results: daily ozone maximum concentration decreases with increasing aerosol optical depth (AOD) in all seasons. Markers are selected cases: AOD = 0.0, 1.0, 2.0, 3.0, 4.0, and 5.0.

3.3. Aerosol Effect Estimation

[24] Ozone precursor relationships have been examined on selected TODC days to minimize meteorological influences. However, the effect of aerosols on radiation has not been accounted for. The rapid economic growth and urbanization in China has led to a significant increase in fossil fuel usage and thereby an increase in aerosol particles (such as soot and sulfate), especially in the east-central region [*Zhao et al.*, 2006]. To obtain an overview of aerosol pollution in Shanghai, MODIS 550 nm AOD data was used. We have obtained 109 valid values from MODIS observation (blue crosses in Figure 8, top), all of which represent average conditions around midday. The aerosol optical depth in Shanghai averages about 1.0, with the highest value of 3.39 on a heavily polluted day and the lowest value of 0.32 under relatively clean conditions. The removal effect of wet and dry deposition and transport from cleaner regions likely explains the relatively clean periods.

[25] Model simulations are conducted to examine aerosol effect on radiation and thereby ozone production under specific chemical conditions. The NCAR-MM model was used to simulate a five day period and the results on the last day after arriving at a stable state were examined. The chemical parameters are based on measurements on TODC days (CO = 1 ppmv, CH4 = 2 ppmv, NOx = 45 ppbv, alkanes = 29.4 ppbv, alkenes = 13.8 ppbv, aromatics = 15.7 ppbv, oxygenated hydrocarbons = 16.2 ppbv). Photolysis rates were calculated for various seasons. The seasonal and diurnal variations of boundary layer height were also considered for each case. In the model, the aerosol is distributed uniformly through the boundary layer and the actinic flux reductions are calculated for the average middle of the boundary layer. The wavelength ranges from 120 nm to 735 nm with an optical depth assumed to scale inversely with the first power of wavelength. The aerosol single scattering albedo (SSA) is assumed to be 0.91 based on the work of *Ramanathan et al.* [2001]. AOD varies from 0.0 to 5.0 at 550 nm. As illustrated in Figure 11, simulated daily ozone maximum concentrations decrease with increasing aerosol optical depth for all seasons. Ozone reduction is especially sensitive to AOD increase under low AOD condition and high solar radiation. These model simulations indicate that aerosol pollution could cause considerable ozone reduction. Therefore the ozone problem could be more severe in the future as a result of ongoing efforts to improve air quality by reducing aerosol pollution.

4. Conclusions

[26] Ground level ozone and its precursors NOx, CO and NMOCs were measured from 15 June 2006 to 14 June 2007 in downtown Shanghai. During the observation period, ozone reaches its maximum in spring instead of summer possibly due to the rainy season (Meiyu period) in the Yangtze River region of China. Seasonally, NOx and CO peak in winter when chemical processes are slower and shallow boundary layers favor accumulation. NOx and CO has a similar double-peak diurnal cycle, indicating that they are mostly of vehicular origin. Average total NMOC concentrations of both 24-hour and morning sampling periods show large day-to-day variability with no apparent seasonal cycle. Aromatics and alkanes are the major components and are nearly equivalent when expressed as ppbC although their fractions change with time. In spring and autumn, aromatics surpass alkanes as the most abundant category. On average, the NMOC composition of Shanghai based on ppbC mixing ratios is similar to other cities with high aromatic levels. Aromatics play a dominant role in Shanghai ozone formation on both the OH-reactivity and MIR scales. Anthropogenic NMOC are major components of the total mixture and are mainly composed of moderate to low reactivity species. In contrast, biogenic NMOC currently have no significant effect on the overall NMOC reactivity in urban Shanghai due to their low concentrations. Traffic emission is not the only important anthropogenic source in urban Shanghai. Other sources including evaporation of solvents, paint from tall buildings, and emissions from the petrochemical industry should be taken into account.

[27] Early morning NMOC/NOx ratios are typically less than 8:1 and averaged about 4:1 during the entire observational period. Under transport limited conditions, almost all NMOC/NOx ratios are in the NMOC-sensitive regime. Model simulations further confirm that ozone photochemical production in urban Shanghai is NMOC-limited. Therefore a more specific NMOC measurement and source apportionment study is needed to develop effective ozone control strategies. Current ground level ozone in urban Shanghai remains at a relatively low level, but could be a much more severe environmental problem in the future unless appropriate control strategies are established. One noteworthy issue is that ozone photochemical production seems to be suppressed by heavy aerosol pollution in Shanghai. The ongoing reduction of aerosol pollution could reduce aerosol impacts on radiation and thus enhanced surface ozone is expected. Even though a policy for limiting car numbers exists in Shanghai, automobiles have increased significantly in the past few years. In the future, rising traffic could give elevated levels of ozone precursors including NMOC. Meanwhile, with Shanghai undergoing persistent rapid urbanization and industrialization, anthro-

pogenic NMOC arising from various sources such as evaporation and industries will also undoubtedly increase. Projects designed to improve vegetation cover will likely lead to more biogenic NMOC emissions in urban Shanghai. Not surprisingly, these changes in ozone precursors would further complicate the highly nonlinear ozone problem in urban Shanghai. Extensive field experiments, establishment of accurate emission inventories, and detailed model simulations are needed to perform a more accurate analysis of photochemical ozone processes in Shanghai and enable the development of strategies for improving air quality in this region.

[28] **Acknowledgments.** This work was funded by the National Natural Science Foundation of China (NSFC) under grants 40875001 and 40705046. The special project of China Meteorological Bureau in 2007, "Research of monitoring and forecast of atmospheric composition and early warning for severe air pollutions during Shanghai EXPO" also supported this work. The National Center for Atmospheric Research is sponsored by the National Science Foundation.

References

Atkinson, R. (1990), Gas-phase tropospheric chemistry of organic compounds: A review, *Atmos. Environ.*, *24A*, 1–41.

Atkinson, R. (2000), Atmospheric chemistry of VOCs and NOx, *Atmos. Environ.*, *34*, 2063–2101.

Baker, A. K., A. J. Beyersdorf, L. A. Doezema, A. Katzenstein, S. Meinardi, I. J. Simpson, D. R. Blake, and F. S. Rowland (2008), Measurements of nonmethane hydrocarbons in 28 United States cities, *Atmos. Environ.*, *42*, 170–182.

Barletta, B., S. Meinardi, I. J. Simpson, S. Zou, F. S. Rowland, and D. R. Blake (2008), Ambient mixing ratios of nonmethane hydrocarbons (NMHCs) in two major urban centers of the Pearl River Delta (PRD) region: Guangzhou and Dongguan, *Atmos. Environ.*, *42*, 4393–4408.

Bell, M., and H. Ellis (2004), Sensitivity analysis of tropospheric ozone to modified biogenic emissions for the Mid-Atlantic region, *Atmos. Environ.*, *38*, 1879–1889.

Bian, H., S. Q. Han, X. X. Tie, M. L. Sun, and A. X. Liu (2007), Evidence of impact of aerosols on surface ozone concentration in Tianjin, China, *Atmos. Environ.*, *41*, 4672–4681.

Bottenheim, J. W., P. C. Brickell, T. F. Dann, D. K. Wang, F. Hopper, A. J. Gallant, K. G. Anlauf, and H. A. Wiebe (1997), Non-methane hydrocarbons and CO during PACIFIC'93, *Atmos. Environ.*, *31*, 2079–2087.

Carter, W. P. L. (1994), Development of ozone reactivity scales for volatile organic compounds, *J. Air Waste Manage. Assoc.*, *44*, 881–899.

Chameides, W. L., et al. (1992), Ozone precursor relationships in the ambient atmosphere, *J. Geophys. Res.*, *97*, 6037–6055.

Chang, C. C., S. J. Lo, J. G. Lo, and J. L. Wang (2003), Analysis of methyl tert-butyl ether in the atmosphere and implications as an exclusive indicator of automobile exhaust, *Atmos. Environ.*, *37*, 4747–4755.

Chang, T. Y., and S. J. Rudy (1990), Ozone-forming potential of organic emissions from alternative-fueled vehicles, *Atmos. Environ.*, *24A*, 2421–2430.

Chang, C. C., T. Y. Chen, C. Y. Lin, C. S. Yuan, and S. C. Liu (2005), Effects of reactive hydrocarbons on ozone formation in southern Taiwan, *Atmos. Environ.*, *39*, 2867–2878.

Civeroloa, K., et al. (2007), Estimating the effects of increased urbanization on surface meteorology and ozone concentrations in the New York City metropolitan region, *Atmos. Environ.*, *41*, 1803–1818.

Committee on Tropospheric Ozone Formation and Measurement (1991), *Rethinking the Ozone Problem in Urban and Regional Air Pollution*, Natl. Acad. Press, Washington, D. C.

Darnall, K. R., A. C. Lloyd, A. M. Winer, and J. N. Pitts Jr. (1976), Reactivity scale for atmospheric hydrocarbons based on reaction with hydroxyl radical, *Environ. Sci. Technol.*, *10*, 692–696.

DeMore, W. B., S. P. Sander, D. M. Golden, R. F. Hampson, M. J. Kurylo, C. J. Howard, A. R. Ravishankara, C. E. Kolb, and M. J. Molina (1997), Chemical kinetics and photochemical data for use in stratospheric modeling: Evaluation number 12, *NASA, JPL Publ. 97-4*.

Derwent, R. G., M. E. Jenkin, S. M. Saunders, and M. J. Pilling (1998), Photochemical ozone creation potentials for organic compounds in northwest Europe calculated with a master chemical mechanism, *Atmos. Environ.*, *32*, 2429–2441.

Dimitriades, B. (1996), Scientific basis for the VOC reactivity issues raised by section 183(e) of the clean air act amendments of 1990, *J. Air Waste Manage. Assoc.*, *46*, 963–970.

Dodge, M. C. (1984), Combined effects of organic reactivity and NMHC/NOx ratio on photochemical oxidant formation—a modeling study, *Atmos. Environ.*, *18*, 1657–1665.

Duan, J. C., J. H. Tan, L. Yang, S. Wu, and J. M. Hao (2008), Concentration, sources and ozone formation potential of volatile organic compounds (VOCs) during ozone episode in Beijing, *Atmos. Res.*, *88*, 25–35.

EPA (2002), 2001 Nonmethane Organic Compounds (NMOC) and Speciated Nonmethane Organic Compounds (SNMOC) monitoring program, final report, EPA Contract 68-D-99-007.

Fehsenfeld, F. C., et al. (1990), Intercomparison of NO_2 measurement techniques, *J. Geophys. Res.*, *95*, 3579–3597.

Geng, F. H., C. S. Zhao, X. Tang, G. L. Lu, and X. X. Tie (2006), Analysis of ozone and VOCs measured in Shanghai: A case study, *Atmos. Environ.*, *41*, 989–1001.

Gery, M. W., and R. R. Crouse (1990), *User's Guide for Executing OZIPR*, Atmospheric Research and Exposure Assessment Lab., Office of Research and Development, U.S. EPA, Research Triangle Park, N. C.

Haagen-Smit, A. J., C. E. Bradley, and M. M. Fox (1953), Ozone formation in photochemical oxidation of organic substances, *Ind. Eng. Chem.*, *45*, 2086–2089.

Herring, J. A., D. A. Jaffe, H. J. Beine, S. Madronich, and D. R. Blake (1997), High-latitude springtime photochemistry: Part II. Sensitivity studies of ozone production, *J. Atmos. Chem.*, *27*, 155–178.

Hidy, G. M. (2000), Ozone process insights from field experiments: Part I. Overview, *Atmos. Environ.*, *34*, 2001–2022.

Jacobson, M. Z. (2002), *Atmospheric Pollution: History, Science and Regulation*, Cambridge Univ. Press, Cambridge.

Jenkin, M. E., and K. C. Clemitshaw (2000), Ozone and other secondary photochemical pollutants: Chemical processes governing their formation in the planetary boundary layer, *Atmos. Environ.*, *34*, 2499–2527.

Jiang, G. F., and J. D. Fast (2004), Modeling the effects of VOC and NOX emission sources on ozone formation in Houston during the TexAQS 2000 field campaign, *Atmos. Environ.*, *38*, 5071–5085.

Madronich, S., and J. G. Calvert (1990), Permutation reactions of organic peroxy radicals in the troposphere, *J. Geophys. Res.*, *95*, 5697–5715.

Madronich, S., and S. Flocke (1998), The role of solar radiation in atmospheric chemistry, in *Handbook of Environmental Chemistry*, edited by P. Boule, pp. 1–26, Springer-Berlin, Heidelberg.

Middleton, P., W. R. Stockwell, and W. P. L. Carter (1990), Aggregation analysis of volatile organic compound emissions for regional modeling, *Atmos. Environ.*, *24A*, 1107–1133.

Moschonas, N., and S. Glavas (1996), C_3-C_{10} hydrocarbons in the atmosphere of Athens, Greece, *Atmos. Environ.*, *30*, 2769–2772.

Murphy, C. F., and D. T. Allen (2005), Hydrocarbon emissions from industrial release events in the Houston-Galveston area and their impact on ozone formation, *Atmos. Environ.*, *39*, 3785–3798.

Na, K. (2006), Determination of VOC source signature of vehicle exhaust in a traffic tunnel, *J. Environ. Manage.*, *81*, 392–398.

Na, K., Y. P. Kim, K. C. Moon, I. Moon, and K. Fung (2001), Concentrations of volatile organic compounds in an industrial area of Korea, *Atmos. Environ.*, *35*, 2747–2756.

Parrish, D. D., and F. C. Fehsenfeld (2000), Methods for gas-phase measurements of ozone, ozone precursors and aerosol precursors, *Atmos. Environ.*, *34*, 1921–1957.

Qian, Q., and D. N. Zhang (1999), Composition and characteristics of NMVOC in ambient air in Shanghai, *Shanghai Environ. Sci.*, *18*(9), 400–403.

Qin, Y., G. S. Tonnesen, and Z. Wang (2004), One-hour and eight-hour average ozone in the California South Coast air quality management district: Trends in peak values and sensitivity to precursors, *Environ. Sci.*, *38*, 2197–2207.

Ramanathan, V., et al. (2001), Indian Ocean Experiment: An integrated analysis of the climate forcing and effects of the great Indo-Asian haze, *J. Geophys. Res.*, *106*, 28,371–28,398.

Russell, A., J. Milford, M. S. Bergin, S. McBride, L. McNair, Y. Yang, W. R. Stockwell, and B. Croes (1995), Urban ozone control and atmospheric reactivity of organic gases, *Science*, *269*, 491–495.

Seinfeld, J. H. (1989), Urban air pollution: State of the science, *Science*, *243*, 745–752.

Seinfeld, J. H., and S. N. Pandis (1998), *Atmospheric Chemistry and Physics: From Air Pollution to Climate Change*, Wiley Interscience, New York.

Sexton, K., and H. Westberg (1984), Nonmethane hydrocarbon composition of urban and rural atmospheres, *Atmos. Environ.*, *18*, 1125–1132.

Shiu, C. J., S. C. Liu, C. C. Chang, J. P. Chen, C. C. K. Chou, C. Y. Lin, and C. Y. Young (2007), Photochemical production of ozone and control strategy for Southern Taiwan, *Atmos. Environ.*, *41*, 9324–9340.

Sillman, S. (1999), The relation between ozone, NOx and hydrocarbons in urban and polluted rural environment, *Atmos. Environ.*, *33*, 1821–1845.

Steinbacher, M., C. Zellweger, B. Schwarzenbach, S. Bugmann, B. Buchmann, C. Ordóñez, A. S. H. Prevot, and C. Hueglin (2007), Nitrogen oxide measurements at rural sites in Switzerland: Bias of conventional measurement techniques, *J. Geophys. Res.*, *112*(D11), D11307, doi:10.1029/2006JD007971.

Stephens, S., S. Madronich, F. Wu, J. B. Olson, R. Ramos, A. Retama, and R. Munoz (2008), Weekly patterns of Mexico City's surface concentrations of CO, NOx, PM10 and O3 during 1986–2007, *Atmos. Chem. Phys.*, *8*, 5313–5325.

Trainer, M., D. D. Parrish, P. D. Goldan, J. Roberts, and F. C. Fehsenfeld (2000), Review of observation-based analysis of the regional factors influencing ozone concentrations, *Atmos. Environ.*, *34*, 2045–2061.

Wakamatsu, S., I. Uno, T. Ohara, and K. L. Schere (1999), A study of the relationship between photochemical ozone and its precursor emissions of nitrogen oxides and hydrocarbons in Tokyo and surrounding areas, *Atmos. Environ.*, *33*, 3097–3108.

Wang, H. X., L. J. Zhou, and X. Y. Tang (2006), Ozone concentrations in rural regions of the Yangtze Delta in China, *J. Atmos. Chem.*, *54*, 255–265.

Ying, Z. M., X. X. Tie, and G. H. Li (2009), Sensitivity of ozone concentrations to diurnal variations of surface emissions in Mexico City: A WRF/Chem modeling study, *Atmos. Environ.*, *43*, 851–859.

Zhang, J., T. Wang, W. L. Chameides, C. Cardelino, J. Kwok, D. R. Blake, A. Ding, and K. L. So (2007), Ozone production and hydrocarbon reactivity in Hong Kong, Southern China, *Atmos. Chem. Phys.*, *7*, 557–573.

Zhao, C. S., L. Peng, A. D. Sun, Y. Qin, H. L. Liu, W. L. Li, and X. J. Zhou (2004), Numerical modeling of tropospheric ozone over Yangtze Delta region, *J. Environ. Sci.*, *24*, 525–533.

Zhao, C. S., X. X. Tie, and Y. Lin (2006), A possible positive feedback of reduction of precipitation and increase in aerosols over eastern central China, *Geophys. Res. Lett.*, *33*, L11814, doi:10.1029/2006GL025959.

F. Geng, L. Peng, X. Tang, J. Xu, Q. Yu, and G. Zhou, Pudong Meteorological Bureau, Shanghai Meteorological Administration, Shanghai 200135, China.

A. Guenther and X. Tie, Atmospheric Chemistry Division, National Center for Atmospheric Research, Boulder, CO 80303, USA.

L. Ran and C. Zhao, Department of Atmospheric Science, School of Physics, Peking University, Beijing 100871, China. (zcs@pku.edu.cn)